

# MODALITY-INCONSISTENT CONTINUAL LEARNING OF MULTIMODAL LARGE LANGUAGE MODELS

## Anonymous authors

Paper under double-blind review

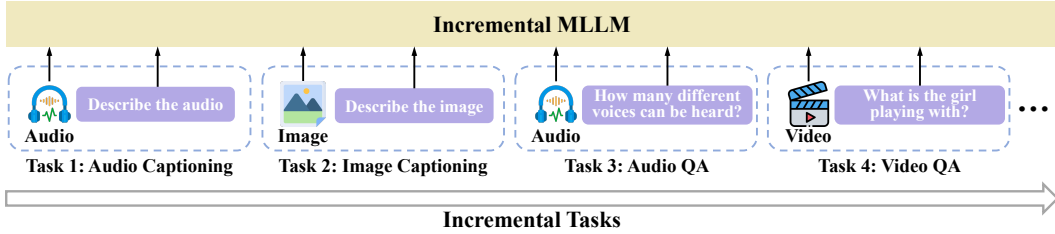


Figure 1: Illustration of our proposed Modality-Inconsistent Continual Learning (MICL), a novel and practical continual learning scenario of Multimodal Large Language Models (MLLMs), where tasks involve inconsistent modalities (image, video, or audio) and varying task types (captioning or question-answering).

## ABSTRACT

In this paper, we introduce Modality-Inconsistent Continual Learning (MICL), a new continual learning scenario for Multimodal Large Language Models (MLLMs) that involves tasks with inconsistent modalities (image, audio, or video) and varying task types (captioning or question-answering). Unlike existing vision-only or modality-incremental settings, MICL combines modality and task type shifts, both of which drive catastrophic forgetting. To address these challenges, we propose MoInCL, which employs a Pseudo Targets Generation Module to mitigate forgetting caused by task type shifts in previously seen modalities. It also incorporates Instruction-based Knowledge Distillation to preserve the model’s ability to handle previously learned modalities when new ones are introduced. We benchmark MICL using a total of six tasks and conduct experiments to validate the effectiveness of our proposed MoInCL. The experimental results highlight the superiority of MoInCL, showing significant improvements over representative and state-of-the-art continual learning baselines.

## 1 INTRODUCTION

Multimodal Large Language Models (MLLMs), leveraging the generative capabilities of LLMs, have demonstrated remarkable performance across diverse modality-specific tasks (Li et al., 2022b; 2023; Zhang et al., 2023b; Liu et al., 2023; Panagopoulou et al., 2023; Liu et al., 2024). MLLMs typically consist of a pre-trained modality encoder, like CLIP (Radford et al., 2021) for visual data, a pre-trained LLM, and a modality adapter that projects modality-specific features into the language token space. During training, the modality encoder is usually frozen to preserve its pre-trained knowledge, while the adapter and, optionally, the LLM are fine-tuned to align cross-modal representations and enhance task performance.

While fine-tuned MLLMs have demonstrated promising performance across various multimodal tasks, including impressive zero-shot capabilities on unseen instructions (He et al., 2023), adapting to novel tasks still requires task-specific fine-tuning. Nevertheless, existing studies (He et al., 2023; Zeng et al., 2024; Zheng et al., 2024) indicate that fine-tuning MLLMs on new tasks can lead to significant performance degradation on previously learned tasks, a phenomenon known as *catastrophic forgetting*, which remains the key challenge in continual learning. To address this issue, several works explore new approaches to enable continual training of MLLMs while mitigating the catastrophic forgetting issue. For instance, He et al. (2023) introduce the continual instruction tuning scenario for multimodal large language models, and propose an adapter-based method

054 to handle it. [Zheng et al. \(2024\)](#) further explore the negative forward transfer problem in continual  
 055 instruction tuning of MLLMs and propose a prompt-based method to mitigate these problems.  
 056 [Cao et al. \(2024\)](#) propose a MLLM-based continual learning framework but mainly focusing on  
 057 class-incremental image classification. While existing methods have demonstrated their abilities in  
 058 alleviating the catastrophic problem in the continual learning scenario of MLLMs, they primarily  
 059 focus on image modality, ignoring more general multimodal scenarios beyond image. Recently, [Yu  
 060 et al. \(2024\)](#) introduced a modality-incremental setting for MLLMs, but treated each modality as a  
 061 single, non-incremental task, ignoring the incremental nature of task types within modalities.

062 To address these issues, in this paper, we introduce Modality-Inconsistent Continual Learning  
 063 (MICL), a novel continual learning scenario for MLLMs. In MICL, different task types, such as  
 064 captioning and question-answering (QA), are introduced incrementally across learning steps incor-  
 065 porated with inconsistent modalities, as illustrated in Fig. 1. Unlike existing incremental learning  
 066 settings of MLLMs, MICL not only highlights the modality-inconsistent (modality-incremental)  
 067 scenario but also emphasizes the potential catastrophic forgetting problem arising from task type  
 068 incrementality combined with modality inconsistency.

069 Moreover, we propose MoInCL (**Modality-Inconsistent Continual Learning**), a novel continual  
 070 learning approach designed to address the MICL problem. By leveraging the generative capabili-  
 071 ties of the LLM backbone, MoInCL introduces a *Pseudo Target Generation Module (PTGM)* to  
 072 handle the task type shifts inherent in the task. Additionally, an *Instruction-based Knowledge Dis-  
 073 tillation (IKD)* constraint for LLM backbone is incorporated to preserve its ability to understand  
 074 modality- and task-aware knowledge, preventing the degradation of its learned capabilities.

075 We evaluate our method across image, audio, and video modalities, combined with captioning and  
 076 question-answering (QA) tasks, resulting in six multimodal incremental tasks (Image Captioning,  
 077 Image QA, Audio Captioning, Audio QA, Video Captioning, and Video QA). Our experiments  
 078 demonstrate that MoInCL significantly outperforms representative and state-of-the-art continual  
 079 learning methods, effectively addressing both modality and task type shifts within MICL. In sum-  
 080 mary, this paper contributes the following:

- 081 • We propose the Modality-Inconsistent Continual Learning, a more general and practical  
 082 continual learning scenario of MLLMs, where different modalities are introduced incre-  
 083 mentally combined with different task types.
- 084 • We propose a novel continual learning approach named MoInCL to tackle the task. In  
 085 MoInCL, a *Pseudo Target Generation Module (PTGM)* is introduced to address the task  
 086 type shift problem of previously learned modalities through incremental steps. Moreover,  
 087 we propose the *Instruction-based Knowledge Distillation (IKD)* constraint to prevent the  
 088 LLM from the forgetting of learned both modality- and task-aware knowledge in old tasks.
- 089 • We benchmark the proposed MICL across three modalities—image, audio, and video—and  
 090 two task types: captioning and question-answering, resulting in six incremental tasks. Ex-  
 091 perimental results demonstrate that our approach, MoInCL, significantly outperforms rep-  
 092 resentative and state-of-the-art continual learning methods, showcasing its effectiveness in  
 093 mitigating catastrophic forgetting from both modality and task type perspectives.

## 095 2 RELATED WORK

### 097 2.1 MULTIMODAL LARGE LANGUAGE MODELS

099 Recent advances have extended Large Language Models (LLMs) to handle multimodal inputs such  
 100 as images, audio, and video. Early work like CLIP ([Radford et al., 2021](#)) demonstrated the effec-  
 101 tiveness of aligning textual and visual representations for zero-shot image classification. Flamingo  
 102 ([Alayrac et al., 2022](#)) further integrated vision encoders with LLMs via cross-attention, signifi-  
 103 cantly improving visual question answering (VQA) and image captioning. Subsequent models like  
 104 BLIP ([Li et al., 2022b](#)) and PaLM-E ([Driess et al., 2023](#)) scaled multimodal pre-training, with  
 105 BLIP using a two-stage training strategy and PaLM-E incorporating embodied reasoning. More  
 106 recently, LLaVA ([Liu et al., 2023](#)), InstructBLIP ([Dai et al., 2023](#)), X-InstructBLIP ([Panagopoulou  
 107 et al., 2023](#)), Audio Flamingo ([Kong et al., 2024](#); [Ghosh et al., 2025](#); [Goel et al., 2025](#)), VideoL-  
 LaMA ([Zhang et al., 2023a](#); [Cheng et al., 2024](#); [Zhang et al., 2025](#)), Qwen-VL ([Wang et al., 2024](#);

108 [Bai et al., 2025](#)), etc., have leveraged instruction tuning to refine the alignment between multimodal  
 109 inputs and language, pushing the boundaries of multimodal reasoning and generation. Despite this  
 110 progress, challenges persist as models scale to new modalities or tasks. Effectively integrating each  
 111 modality without degrading performance on others remains a key issue. Moreover, robust continual  
 112 learning strategies are crucial to prevent catastrophic forgetting and maintain knowledge across both  
 113 previously learned and newly introduced modalities as new modalities or task types are integrated.  
 114

## 115 2.2 CONTINUAL LEARNING 116

117 Continual learning aims to enable models to learn incrementally while retaining previously acquired  
 118 knowledge. Regularization-based methods, such as Elastic Weight Consolidation (EWC) ([Kirk-](#)  
 119 [patrick et al., 2017](#)), assign importance to model parameters to prevent drastic updates ([Kim et al.,](#)  
 120 [2023](#)). Knowledge distillation (KD) ([Li & Hoiem, 2017](#); [Rebuffi et al., 2017](#); [Pian et al., 2023](#); [Mo](#)  
 121 [et al., 2023](#); [Ahn et al., 2021](#); [Douillard et al., 2020](#)) and memory replay ([Rebuffi et al., 2017](#); [Pian](#)  
 122 [et al., 2024](#); [Chaudhry et al., 2019](#); [Lopez-Paz & Ranzato, 2017](#)) are other common strategies, where  
 123 KD-based methods preserve past learned knowledge by aligning the predictions or internal features  
 124 of a new model with those of an older one, and memory replay-based methods utilize a small mem-  
 125 ory set to store samples from old tasks, allowing the model to review a small number of old data  
 126 while training on the current task ([Rebuffi et al., 2017](#); [Pian et al., 2024](#); [Chaudhry et al., 2019](#);  
 127 [Lopez-Paz & Ranzato, 2017](#)). Pseudo-rehearsal approaches ([Odena et al., 2017](#); [Ostapenko et al.,](#)  
 128 [2019](#)) take this a step further by generating synthetic examples via a generative model, reducing the  
 129 need to store large amounts of data.  
 130

130 For MLLMs, where multiple modalities (e.g., images, audio, video) interact with language mod-  
 131 els, catastrophic forgetting is especially severe. Recent adapter-based continual instruction tun-  
 132 ing ([He et al., 2023](#)) and prompt-based strategies ([Zheng et al., 2024](#)) help retain previously learned  
 133 knowledge. HiDe-LLaVA ([Guo et al., 2025](#)) proposes a hierarchical decoupling strategy to sep-  
 134 arate instruction and perception components, allowing better task adaptation. SEFE ([Chen et al.,](#)  
 135 [2025](#)) addresses forgetting by distinguishing between essential and superficial knowledge in con-  
 136 tinual instruction tuning. CL-MoE ([Huai et al., 2025](#)) introduces a dual momentum mixture-of-  
 137 experts framework for continual visual question answering. However, these approaches mainly  
 138 target image-text modalities. A modality-incremental scenario ([Yu et al., 2024](#)) has been explored,  
 139 treating each modality as a separate task. However, it does not fully address evolving task types  
 140 within each modality. To tackle this gap, we propose a new Modality-Inconsistent Continual Learn-  
 141 ing (MICL) scenario along with a novel approach to handle it effectively.  
 142

## 143 3 METHOD

### 144 3.1 PROBLEM FORMULATION

145 In this subsection, we formalize the definition of our proposed Modality-Inconsistent Continual  
 146 Learning (MICL). Given a sequence of  $T$  tasks  $\{\mathcal{T}_1, \mathcal{T}_2, \dots, \mathcal{T}_T\}$ , MICL aims to train the Multimodal  
 147 Large Language Model (MLLM)  $\mathcal{F}_\Theta$  with parameters  $\Theta$  across these tasks incrementally. For the  
 148  $i$ -th task  $\mathcal{T}_i$ , we have  $\mathcal{T}_i = \{(\mathbf{x}_{i,j}, \mathbf{t}_{i,j}, \mathbf{y}_{i,j})_{j=1}^{n_i}, M_i, P_i\}$ , where  $M_i$  and  $P_i$  denote the modality and  
 149 task type of task  $\mathcal{T}_i$ , respectively.  $\mathbf{x}_{i,j}$ ,  $\mathbf{t}_{i,j}$ , and  $\mathbf{y}_{i,j}$  present the modality’s input data, the input  
 150 text, and the target text of the  $j$ -th data sample of task  $\mathcal{T}_i$ . In our setting, the input text  $\mathbf{t}_{i,j}$  varies  
 151 depending on the task type. For captioning tasks, it may consist of a simple instruction, such as  
 152 “Describe the image/video/audio.” For question-answering (QA) tasks, the input text  
 153 consists of sample-specific questions tailored to each instance. Moreover, the target text  $\mathbf{y}_{i,j}$  typi-  
 154 cally consists of detailed description sentences for captioning tasks, while for QA tasks, it is usually  
 155 limited to a few answer words. *Please note that, the output  $\mathbf{y}_{i,j}$  is always a text sequence, consistent*  
 156 *with the design of LLMs and MLLMs, which generate natural language outputs across diverse tasks.*  
 157 *Tasks with non-textual outputs (e.g., image or video generation) are beyond the scope of our current*  
 158 *formulation, as they typically require fundamentally different architectures and objectives.* We de-  
 159 fine  $\mathcal{D}_i = \{(\mathbf{x}_{i,j}, \mathbf{t}_{i,j}, \mathbf{y}_{i,j})_{j=1}^{n_i}\}$  as the available training data when training the model  $\mathcal{F}_\Theta$  on task  
 160  $\mathcal{T}_i$ . Following the settings in modality-incremental learning ([Yu et al., 2024](#)), we do not include the  
 161 memory set for replay in our MICL scenario, resulting in a memory-free continual learning setting.  
 162

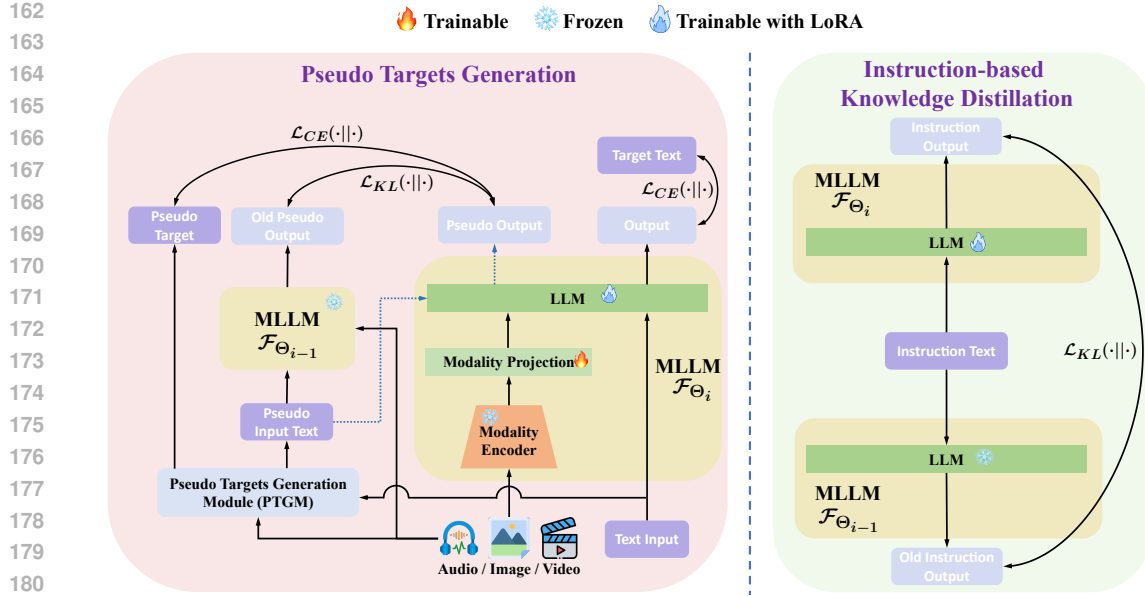


Figure 2: Overview of our proposed MoInCL, which mainly consists of a Multimodal Large Language Model (MLLM), a Pseudo Target Generation Module (PTGM), and a Instruction-based Knowledge Distillation (IKD). The red fire icon denotes the component is trainable in the current task, and the snowflake icon denotes the component is frozen during the training of the current task, while the blue fire icon means the associate component is trainable with LoRA (Hu et al., 2022) when training on the current task.

In summary, the training process on an incremental task  $\mathcal{T}_i$  can be presented as:

$$\Theta_i = \arg \min_{\Theta_{i-1}} \mathbb{E}_{(\mathbf{x}, \mathbf{t}, \mathbf{y}) \sim \mathcal{D}_i} [\mathcal{L}(\mathcal{F}_{\Theta_{i-1}}(\mathbf{x}, \mathbf{t}), \mathbf{y})], \quad (1)$$

where  $\mathcal{L}$  denotes the cross-entropy loss function between the generated results and the target text for training the MLLM.

Please note that, in this work, we focus on two task types (captioning and question-answering) since they are among the most commonly studied in multimodal and continual learning scenarios (He et al., 2023; Yu et al., 2024). Following common practice, we adopted these tasks to establish benchmarks for comparison. Additionally, most of multimodal task types such as audio-visual event localization, vision-language navigation, etc, can often be reformulated into question-answering tasks, making these two task types a natural choice in our setting.

### 3.2 FRAMEWORK OVERVIEW

To address our proposed Modality-Inconsistent Continual Learning (MICL), we introduce a novel continual learning method, **MoInCL**, as illustrated in Fig. 2. MoInCL primarily comprises a Pseudo Target Generation Module (PTGM) and an Instruction-based Knowledge Distillation (IKD) constraint. For the MLLM, we adopt the LLaVA-like (Liu et al., 2023) architecture, which contains the same core components as LLaVA (modality encoder, projection layer, and LLM). However, we do not directly use LLaVA or its pre-trained parameters, as it is designed to process only the visual modality, and its visual pre-training could introduce biases in the context of continual learning. Please note that, for fair comparison, all the baseline methods use the same model architecture as our method. During training, the modality encoders remain frozen, while the LLM is fine-tuned using LoRA (Hu et al., 2022).

### 3.3 PSEUDO TARGET GENERATION MODULE

We now describe the Pseudo Target Generation Module (PTGM). Our key motivation is to leverage the text generation capability of the LLM component in the MLLM to address the task type shift challenge in continual learning. PTGM generates input and target text for different task types based

on the modality input data of the current task. By utilizing the generated pseudo input text and pseudo targets, the model can effectively handle both the current task type and previously learned task types within the current modality.

In our PTGM, we maintain a set  $LM = \{\}$  to represent all learned modalities. For example,  $LM = \{\text{"image"}, \text{"audio"}\}$  indicates that the model has been trained on tasks involving image or audio modalities. And for learned modalities, we maintain a modality-specific set  $LT_M = \{\}$  to denote the learned task types of modality  $M$ . For instance,  $LT_{\text{image}} = \{\text{"captioning"}\}$  if only image captioning task has been learned for image modality. Since different task types have distinct forms, the pseudo target generation process varies accordingly for each task type. Specifically, for a current task  $\mathcal{T}_i$  with the modality of  $M_i$ , if  $M_i$  is a learned modality, *i.e.*  $M_i \in LM$ , the PTGM will be used to generate pseudo targets for task types within  $LT_{M_i}$ . If  $\text{"captioning"} \in LT_{M_i}$ , the pseudo input text should be a simple instruction guiding the model to generate a description of the input data. In this case, the pseudo input text generation process can be implemented by automatically filling the template to produce the result  $\text{"Describe the } M_i\text{"}$ . On the other hand, if  $\text{"QA"} \in LT_{M_i}$ , directly applying a template is not suitable, as the pseudo QA pair should be specifically tailored to the modality's data rather than relying on generic templates. To overcome this issue, we utilize the generation ability of the LLM to generate the pseudo QA pair from the caption text of the current modality's data. Please note that in our MICL scenario, the task types considered are captioning and question-answering. Therefore, when generating pseudo QA pairs, the current task should correspond to the captioning task of the current modality. To generate QA pairs from captions, we employ a three-round generation process by prompting the pre-trained LLM component of the MLLM  $\mathcal{F}$ . Details of this process can be found in the Appendix. In summary, we use the following formulation to denote the pseudo target generation process:

$$\begin{aligned} \tilde{\mathbf{t}}, \tilde{\mathbf{y}} &= PTGM(\mathbf{x}, \mathbf{y}, p), \\ \text{s.t. } M_i &\in LM, P_i \notin LT_{M_i}, \end{aligned} \quad (2)$$

where  $p \in LT_{M_i}$  is a learned task type of modality  $M_i$  (please note that  $p \neq P_i$ ),  $\tilde{\mathbf{t}}$  and  $\tilde{\mathbf{y}}$  denote the generated pseudo input text and pseudo target, respectively.  $\mathbf{x}$  and  $\mathbf{y}$  are the modality data and target text sampled from  $\mathcal{D}_i$ . Please note that only  $\mathbf{x}$  is used for generating pseudo targets, while only  $\mathbf{y}$  is utilized for generating pseudo QA pairs.

After obtaining the pseudo input text and pseudo target, a dual consistency constraint is applied between (1) the pseudo outputs of the current model  $\mathcal{F}_{\Theta_i}$  and the old model  $\mathcal{F}_{\Theta_{i-1}}$ , and (2) the pseudo target and the pseudo output of the current model. This process is formulated as:

$$\begin{aligned} \mathcal{L}_p &= \mathbb{E}_{(\mathbf{x}, \mathbf{t}) \sim \mathcal{D}_i} \left[ \lambda_i \mathcal{L}_{CE}(\hat{\mathbf{y}}' \parallel \tilde{\mathbf{y}}) + \lambda'_i \mathcal{L}_{KL}(\hat{\mathbf{y}}' \parallel \hat{\mathbf{y}}'_o) \right], \\ \text{s.t. } \hat{\mathbf{y}}' &= \mathcal{F}_{\Theta_i}(\mathbf{x}, \tilde{\mathbf{t}}), \hat{\mathbf{y}}'_o = \mathcal{F}_{\Theta_{i-1}}(\mathbf{x}, \tilde{\mathbf{t}}), \end{aligned} \quad (3)$$

where  $\hat{\mathbf{y}}'_o$  and  $\hat{\mathbf{y}}'$  denote the pseudo output from the old model and current model, respectively.  $\lambda_i$  and  $\lambda'_i$  present the weights to balance the two loss values for task  $\mathcal{T}_i$ .

### 3.4 INSTRUCTION-BASED KNOWLEDGE DISTILLATION

In the previous subsection, we introduced the proposed PTGM to address the task type shift problem in the MICL scenario. However, when new modalities are introduced, the model faces a modality shift, leading to catastrophic forgetting of previously learned modalities. Additionally, as the PTGM generates pseudo targets only for seen modalities, the task type shift problem persists when training on tasks involving novel modalities. Furthermore, different modalities do *not* share the modality encoder or the modality projection, meaning that the shift problems primarily arise from updates to the LLM component in the MLLM. This results in the degradation of the LLM's ability to handle previously learned modalities. To address these issues, we propose Instruction-based Knowledge Distillation (IKD), a text instruction-based constraint designed to prevent the LLM from forgetting its learned capabilities in dealing with old modalities. Specifically, as illustrated in Fig. 2, IKD aligns the outputs of the LLM component from both the old and current models by applying a consistency loss, *i.e.* KL divergence, on their responses to the same text instruction input. In this way, instead of merely learning to handle tasks from new modalities, the current LLM's generative ability is also aligned with that of the previous LLM, thereby mitigating degradation in its ability to handle previously learned modalities. To achieve this, we introduce a pure text instruction set within IKD,

which is maintained throughout the incremental steps. Since this pure text instruction set contains only text and no modality-specific data, it is not considered part of any multimodal tasks in our MICL scenario. As a result, maintaining this set does not violate the continual learning constraint that prohibits access to data from previous tasks during future tasks. This process can be formulated as:

$$\mathcal{L}_{ins.} = \mathbb{E}_{t' \sim \mathcal{I}} \left[ \mathcal{L}_{KL}(f_{\theta_i}(t') || f_{\theta_{i-1}}(t')) \right], \quad (4)$$

where  $\mathcal{I}$  denotes the pure text instruction set,  $f_{\theta_i}$  and  $f_{\theta_{i-1}}$  denote the LLM component of the  $\mathcal{F}_{\Theta_i}$  and  $\mathcal{F}_{\Theta_{i-1}}$ , respectively.

### 3.5 OVERALL TRAINING TARGET

Above, we present our proposed Pseudo Target Generation Module (PTGM) and Instruction-based Knowledge Distillation (IKD) constraint. When training on a current task  $\mathcal{T}_i$ , we have the main loss function:

$$\begin{aligned} \mathcal{L}_{main} &= \mathbb{E}_{(\mathbf{x}, \mathbf{t}, \mathbf{y}) \sim \mathcal{D}_i} \left[ \mathcal{L}_{CE}(\hat{\mathbf{y}} || \mathbf{y}) \right], \\ &\text{s.t. } \hat{\mathbf{y}} = \mathcal{F}_{\Theta_i}(\mathbf{x}, \mathbf{t}), \end{aligned} \quad (5)$$

where  $\hat{\mathbf{y}}$  is the output of the output of the current model  $\mathcal{F}_{\Theta_i}$  by taking data samples from current task's training data  $\mathcal{D}_i$  as input.

Finally, in our overall training target, the dual consistency constraint for generated pseudo targets  $\mathcal{L}_{pseudo}$  and the IKD constraint  $\mathcal{L}_{ins.}$  are combined with the main training loss of task  $\mathcal{T}_i$ :

$$\mathcal{L} = \mathcal{L}_{main} + \mathcal{L}_{p.} + \mathcal{L}_{ins.} \quad (6)$$

Additionally, inspired by the parameters/weights fusion mechanism proposed in existing works (Xiao et al., 2023; Sun et al., 2024), which have demonstrated effectiveness in preserving learned knowledge from previous tasks by applying a weighted sum between the old and current models' parameters/weights, we also adopt the parameters fusion mechanism on the LLM component of the MLLM to further prevent it from forgetting the capabilities of handling previously learned modalities, which can be denoted as:

$$\theta_i = \alpha_i \theta_i + (1 - \alpha_i) \theta_{i-1}, \quad (7)$$

where  $\theta$  denotes the parameters of the LLM component of the MLLM,  $\alpha_i$  is the weight for balancing the two groups of parameters. For the overall algorithm of our MoInCL, please refer to the Appendix.

## 4 EXPERIMENTS

### 4.1 EXPERIMENTAL SETUP

**Dataset.** In our proposed Modality-Inconsistent Continual Learning (MICL), we include six tasks: Image Captioning, Image QA, Audio Captioning, Audio QA, Video Captioning, and Video QA. Each task is represented by a commonly used dataset. Specifically, we use the Flickr30K (Young et al., 2014) dataset for the Image Captioning task, the OK-VQA (Marino et al., 2019) dataset for the Image QA task, the AudioCaps (Kim et al., 2019) dataset for the Audio Captioning task, the Clotho-AQA (Lipping et al., 2022) dataset for the Audio QA task, the MSR-VTT (Xu et al., 2016) dataset for the Video Captioning task, and the MSVD-QA (Xu et al., 2017) dataset for the Video QA task. More dataset details are provided in the Appendix.

**Baselines.** In our experiments, we compare our proposed MoInCL with the following continual learning methods: Fine-tuning, LwF (Li & Hoiem, 2017), EWC (Kirkpatrick et al., 2017), EWF (Xiao et al., 2023), PathWeave (Yu et al., 2024), and BECAME (Li et al., 2025). Among these, LwF, EWC, EWF, and BECAME are representative general continual learning methods, while PathWeave is the most recent state-of-the-art continual learning method designed for MLLMs, which involves a modality-aware adapter-in-adapter mechanism to address the modality-shift problem in

324  
325 Table 1: Results on the two task orders for different methods. Bold values indicate the best results  
326 in each column, while underlined values represent the second-best results in each column.

327 Methods	328 Order 1			329 Order 2		
	330 Avg. CIDEr $\uparrow$	331 Avg. Acc. $\uparrow$	332 Avg. Forget. $\downarrow$	333 Avg. CIDEr $\uparrow$	334 Avg. Acc. $\uparrow$	335 Avg. Forget. $\downarrow$
Fine-tuning	30.64	<b>40.58</b>	41.17%	10.82	37.01	65.56%
LwF (Li & Hoiem, 2017)	34.80	40.21	39.26%	12.37	38.79	61.84%
EWC (Kirkpatrick et al., 2017)	<u>39.06</u>	37.04	<u>38.79%</u>	9.92	37.65	66.40%
EWF (Xiao et al., 2023)	24.59	36.34	<u>48.55%</u>	<u>13.92</u>	<b>45.85</b>	<u>46.64%</u>
PathWeave (Yu et al., 2024)	34.20	36.19	44.36%	11.11	41.13	61.47%
BECAME (Li et al., 2025)	24.36	38.50	46.96%	10.61	43.20	54.10%
<b>MoInCL (Ours)</b>	<b>55.31</b>	<b>42.29</b>	<b>14.21%</b>	<b>51.13</b>	<b>45.22</b>	<b>8.93%</b>
Upper Bound (Joint training)	66.69	48.97	-	66.69	48.97	-

336 modality-incremental learning of MLLMs. Please note that, for a fair comparison, all baseline meth-  
337 ods use the same model architecture as our approach, including the Large Language Model (LLM)  
338 component. We also conduct the experiment of joint training with all tasks as the Upper-Bound.

339 **Evaluation Metrics.** Following Panagopoulou et al. (2023), we use the CIDEr score (Vedantam  
340 et al., 2015) and prediction accuracy as evaluation metrics to evaluate captioning tasks and QA tasks,  
341 respectively. For all baselines and our method, we report the average final performance across all  
342 learned tasks, *i.e.*, the average performance of all tasks after completing the training of the final task.  
343 Since captioning and QA tasks use different evaluation metrics, we separately report the average  
344 final performance for each task type: the average final CIDEr score for captioning tasks and the  
345 average final accuracy for QA tasks. We formulate them as:

$$346 \quad \text{Avg. CIDEr} = \frac{1}{N_{cap.}} \sum_{i=1}^T c_i^T, \quad (8)$$

$$349 \quad \text{s.t. } P_i = \text{"Captioning"},$$

351 where  $N_{cap.}$  denotes the number of captioning tasks,  $c_i^T$  denotes the CIDEr score of task  $\mathcal{T}_i$  after  
352 completing the training of task  $\mathcal{T}_T$  if task  $\mathcal{T}_i$  is a captioning task. Similarly, the average final accuracy  
353 can be formulated as:

$$354 \quad \text{Avg. Acc.} = \frac{1}{N_{QA}} \sum_{i=1}^T a_i^T, \quad (9)$$

$$357 \quad \text{s.t. } P_i = \text{"QA"},$$

358 where  $N_{QA}$  denotes the number of QA tasks,  $a_i^T$  denotes the accuracy of task  $\mathcal{T}_i$  after completing  
359 the training of task  $\mathcal{T}_T$  if task  $\mathcal{T}_i$  is a QA task. Furthermore, to evaluate the anti-forgetting capability  
360 of each method, we propose two metrics: the forgetting ratio and the average forgetting ratio. The  
361 forgetting ratio measures the proportion of performance drop for each task after completing the  
362 training of the final task, while the average forgetting ratio represents the mean forgetting ratio  
363 across all tasks, which can be formulated as:

$$364 \quad \text{Forget.}_i = (s_i^i - s_i^T) / s_i^i, \quad (10)$$

$$367 \quad \text{Avg. Forget.} = \frac{1}{T} \sum_{i=1}^T \text{Forget.}_i$$

369 where  $s_i^i$  and  $s_i^T$  denotes the testing score of task  $\mathcal{T}_i$  after the training of task  $\mathcal{T}_i$  and  $\mathcal{T}_T$ , respectively.

## 371 4.2 EXPERIMENTAL COMPARISON

373 We conduct experiments using two random task orders. For **Order 1**, the tasks are arranged as: *Au-*  
374 *dio Captioning*  $\rightarrow$  *Image Captioning*  $\rightarrow$  *Video QA*  $\rightarrow$  *Audio QA*  $\rightarrow$  *Image QA*  $\rightarrow$  *Video Captioning*.  
375 For **Order 2**, the task sequence is: *Image Captioning*  $\rightarrow$  *Video Captioning*  $\rightarrow$  *Video QA*  $\rightarrow$  *Image*  
376 *QA*  $\rightarrow$  *Audio Captioning*  $\rightarrow$  *Audio QA*. Additional experimental results on more task orders are pro-  
377 vided in Appendix A.8, where we demonstrate that our framework can handle highly challenging  
task orders involving severe modality and task shifts.

378  
 379 Table 2: Detailed testing results of the first three tasks of Order 2. The evaluation metric used for the  
 380 Flickr30K and MSR-VTT datasets is CIDEr score, while that for the MSVD-QA dataset is accuracy.

Methods	Flickr30k	MSR-VTT	MSVD-QA
Fine-tuning	Step 1 77.50	-	-
	Step 2 64.04	48.03	-
	Step 3 12.12	8.64	46.20
LwF (Li & Hoiem, 2017)	Step 1 77.50	-	-
	Step 2 53.87	48.70	-
	Step 3 10.20	7.80	47.64
EWC (Kirkpatrick et al., 2017)	Step 1 77.50	-	-
	Step 2 62.65	47.73	-
	Step 3 10.45	9.66	45.79
EWF (Xiao et al., 2023)	Step 1 77.50	-	-
	Step 2 69.16	45.30	-
	Step 3 56.10	9.69	45.33
PathWeave (Yu et al., 2024)	Step 1 77.22	-	-
	Step 2 53.60	50.01	-
	Step 3 7.36	8.35	47.87
BECAME (Li et al., 2025)	Step 1 77.50	-	-
	Step 2 77.22	47.64	-
	Step 3 52.16	9.82	47.35
MoInCL (Ours)	Step 1 77.50	-	-
	Step 2 73.59	48.03	-
	Step 3 70.88	48.34	43.11

405  
 406 The main results are shown in Tab. 1. We can see that our proposed MoInCL achieves state-of-the-  
 407 art performance compared to all baseline methods. Except the average final accuracy of the Order 2,  
 408 our method has the best performance on all three metrics across both orders. Specifically, in Order  
 409 1, our method surpasses the best baseline results by **16.25**, **1.71**, and **24.58** in terms of average  
 410 final CIDEr score, average final accuracy, and average forgetting ratio, respectively. In Order 2, our  
 411 method outperforms the best baseline results by **37.21** and **37.71** for average final CIDEr score and  
 412 average forgetting ratio, respectively.

413 The testing results of the first three incremental tasks (Image Captioning → Video Captioning →  
 414 Video QA) are shown in Tab. 2. From these results, we observe that when the modality shift occurs  
 415 from the Image Captioning task to the Video Captioning task, the performance of the previous task  
 416 (Image Captioning) drops significantly across all baseline methods, with CIDEr score reductions  
 417 ranging from 8.34 to 23.63. Additionally, when the task type shift occurs from the Video Cap-  
 418 tioning task to the Video QA task, the performance of the previous task (Video Captioning) also  
 419 decreases significantly, with CIDEr score reductions ranging from 35.61 to 41.66. These results  
 420 further validate our insight that both modality shift and task type shift directly contribute to the  
 421 catastrophic forgetting problem, underscoring the core challenges of our proposed MICL scenario.  
 422 For our method, the performance drop for the Image Captioning task is only **3.91** when the modality  
 423 shift occurs. Moreover, we observe that the performance of the Video Captioning task improves  
 424 after training on the Video QA task which introduces the task type shift issue. These findings further  
 425 highlight the effectiveness of our method in mitigating the catastrophic forgetting problem in MICL  
 426 by addressing both modality shift and task type shift challenges. For detailed results of each task  
 427 and qualitative analysis, please refer to Sec. A.9, A.10 and A.11 in Appendix.

#### 428 4.3 ABLATION STUDIES

430 To further assess the effectiveness of each key component in our proposed MoInCL, we conduct  
 431 ablation studies on the Pseudo Target Generation Module (PTGM) and Instruction-based Knowledge  
 Distillation (IKD) across two random task orders. The experimental results, presented in Tab. 3,

432  
 433 Table 3: Ablation results on the two task orders on each key component of our MoInCL. Bold values  
 434 indicate the best results in each column, while underlined values represent the second-best results in  
 435 each column.

436 Methods	Order 1			Order 2		
	Avg. CIDEr $\uparrow$	Avg. Acc. $\uparrow$	Avg. Forget. $\downarrow$	Avg. CIDEr $\uparrow$	Avg. Acc. $\uparrow$	Avg. Forget. $\downarrow$
437 MoInCL w/o PTGM	26.61	37.18	45.64%	9.95	<b>47.51</b>	49.62%
438 MoInCL w/o IKD	53.33	40.69	17.82%	49.32	43.40	13.03%
439 MoInCL	<b>55.31</b>	<b>42.29</b>	<b>14.21%</b>	<b>51.13</b>	<u>45.22</u>	<u>8.93%</u>

440  
 441 clearly demonstrate that removing either PTGM or IKD leads to a performance drop in both task  
 442 orders. This highlights the significance of each component in our framework.  
 443

#### 444 4.4 RESULTS ANALYSIS

445  
 446 We provide a more detailed analysis of the experimental results, specifically examining why the  
 447 average accuracy of QA tasks in Order 2 does not achieve the best performance. In Order 2, the last  
 448 four tasks follow the sequence: *Video QA*  $\rightarrow$  *Image QA*  $\rightarrow$  *Audio Captioning*  $\rightarrow$  *Audio QA*, where  
 449 QA tasks dominate. Consequently, the task type shift problem has a greater impact on captioning  
 450 tasks than on QA tasks. For the baseline methods, as they focus less on addressing the task type  
 451 shift problem, they prioritize QA tasks in the later stages of Order 2 rather than preserving knowl-  
 452 edge from earlier tasks. This explains why most baseline methods perform better on QA tasks in  
 453 Order 2 compared to Order 1. Nevertheless, our MoInCL still outperforms all other baselines in  
 454 terms of average accuracy of QA tasks, except for EWF, where the difference is marginal. Addi-  
 455 tionally, MoInCL exhibits a lower average forgetting ratio compared to all baselines in both orders,  
 456 and achieves lower forgetting ratio on each single task. Moreover, MoInCL maintains more stable  
 457 performance across both task orders, further demonstrating the robustness of our method.  
 458

## 459 5 CONCLUSION

460  
 461 In this paper, we explore the Modality-Inconsistent Continual Learning (MICL), a novel and prac-  
 462 tical continual learning scenario of Multimodal Large Language Models (MLLMs). To address the  
 463 introduced MICL, we propose MoInCL, which incorporates a Pseudo Targets Generation Modul  
 464 and an Instruction-based Knowledge Distillation constraint to mitigate the catastrophic forgetting  
 465 caused by the inherent task type shift and modality shift problem in the context of MICL. Experi-  
 466 ments on six multimodal incremental tasks demonstrate the effectiveness of our proposed MoInCL.  
 467 This paper introduces a new direction for the continual learning of MLLMs.

468 **Broader Impact.** Our proposed continual modality-inconsistent continual learning allows the  
 469 MLLMs to adapt to new modalities and task types without full retraining, which could enhance  
 470 efficiency and privacy by reducing the need to transmit and store sensitive data.

## 471 LIMITATIONS

472  
 473 Our Modality-Inconsistent Continual Learning (MICL) introduces a novel and practical continual  
 474 learning scenario by incorporating inconsistent modalities and varying task types across incremental  
 475 tasks. However, the scope of our work is constrained by the limited number of modalities (audio,  
 476 image, and video) and task types (captioning and question-answering) included in the experiments.  
 477 This restricts the generalizability of MICL to scenarios involving a broader range of modalities and  
 478 task types. Another limitation lies in the pseudo QA pairs generated by PTGM, which may not  
 479 fully capture the complete answer space of prior QA tasks, leading to incomplete supervision when  
 480 mitigating the task type shift from QA to captioning tasks. These imperfect pseudo targets may thus  
 481 still hinder a full resolution of the task type shift problem.

482  
 483 In the future, we plan to enhance our MICL framework by incorporating additional modalities,  
 484 such as depth, 3D, or even joint inputs like joint audio-visual modalities. We also aim to introduce  
 485 a broader range of task types, such as reasoning, grounding, decision-making, etc. Furthermore,  
 486 scaling up MICL to larger datasets within each task is also a key objective to better enable the model  
 487 to address the complexity and diversity of real-world multimodal tasks in continual learning.

486 REFERENCES  
487

488 Josh Achiam, Steven Adler, Sandhini Agarwal, Lama Ahmad, Ilge Akkaya, Florencia Leoni Ale-  
489 man, Diogo Almeida, Janko Altenschmidt, Sam Altman, Shyamal Anadkat, et al. Gpt-4 technical  
490 report. *arXiv preprint arXiv:2303.08774*, 2023.

491 Hongjoon Ahn, Jihwan Kwak, Subin Lim, Hyeonsu Bang, Hyojun Kim, and Taesup Moon. Ss-  
492 il: Separated softmax for incremental learning. In *Proceedings of the IEEE/CVF International*  
493 *conference on computer vision*, pp. 844–853, 2021.

494 Jean-Baptiste Alayrac, Jeff Donahue, Pauline Luc, Antoine Miech, Iain Barr, Yana Hasson, Karel  
495 Lenc, Arthur Mensch, Katherine Millican, Malcolm Reynolds, et al. Flamingo: a visual language  
496 model for few-shot learning. *Advances in neural information processing systems*, 35:23716–  
497 23736, 2022.

498 Shuai Bai, Keqin Chen, Xuejing Liu, Jialin Wang, Wenbin Ge, Sibo Song, Kai Dang, Peng Wang,  
499 Shijie Wang, Jun Tang, et al. Qwen2.5-vl technical report. *arXiv preprint arXiv:2502.13923*,  
500 2025.

502 Xusheng Cao, Haori Lu, Linlan Huang, Xialei Liu, and Ming-Ming Cheng. Generative multi-modal  
503 models are good class incremental learners. In *Proceedings of the IEEE/CVF Conference on*  
504 *Computer Vision and Pattern Recognition*, pp. 28706–28717, 2024.

505 Arslan Chaudhry, Marcus Rohrbach, Mohamed Elhoseiny, Thalaiyasingam Ajanthan, Puneet K  
506 Dokania, Philip HS Torr, and Marc’Aurelio Ranzato. On tiny episodic memories in continual  
507 learning. *arXiv preprint arXiv:1902.10486*, 2019.

509 Jinpeng Chen, Runmin Cong, Yuzhi Zhao, Hongzheng Yang, Guangneng Hu, Horace Ip, and Sam  
510 Kwong. SEFE: Superficial and essential forgetting eliminator for multimodal continual instruc-  
511 tion tuning. In *Forty-second International Conference on Machine Learning*, 2025.

513 Sanyuan Chen, Yu Wu, Chengyi Wang, Shujie Liu, Daniel Tompkins, Zhuo Chen, Wanxiang Che,  
514 Xiangzhan Yu, and Furu Wei. Beats: Audio pre-training with acoustic tokenizers. In Andreas  
515 Krause, Emma Brunskill, Kyunghyun Cho, Barbara Engelhardt, Sivan Sabato, and Jonathan Scar-  
516 lett (eds.), *International Conference on Machine Learning*, volume 202, pp. 5178–5193. PMLR,  
517 2023.

518 Zesen Cheng, Sicong Leng, Hang Zhang, Yifei Xin, Xin Li, Guanzheng Chen, Yongxin Zhu, Wenqi  
519 Zhang, Ziyang Luo, Deli Zhao, et al. Videollama 2: Advancing spatial-temporal modeling and  
520 audio understanding in video-llms. *arXiv preprint arXiv:2406.07476*, 2024.

521 Wenliang Dai, Junnan Li, Dongxu Li, Anthony Tiong, Junqi Zhao, Weisheng Wang, Boyang Li,  
522 Pascale Fung, and Steven Hoi. InstructBLIP: Towards general-purpose vision-language models  
523 with instruction tuning. In *Thirty-seventh Conference on Neural Information Processing Systems*,  
524 2023.

526 Arthur Douillard, Matthieu Cord, Charles Ollion, Thomas Robert, and Eduardo Valle. Podnet:  
527 Pooled outputs distillation for small-tasks incremental learning. In *Computer vision–ECCV 2020:*  
528 *16th European conference, Glasgow, UK, August 23–28, 2020, proceedings, part XX 16*, pp. 86–  
529 102. Springer, 2020.

530 Danny Driess, Fei Xia, Mehdi SM Sajjadi, Corey Lynch, Aakanksha Chowdhery, Brian Ichter,  
531 Ayzaan Wahid, Jonathan Tompson, Quan Vuong, Tianhe Yu, et al. Palm-e: An embodied multi-  
532 modal language model. *arXiv preprint arXiv:2303.03378*, 2023.

533 Abhimanyu Dubey, Abhinav Jauhri, Abhinav Pandey, Abhishek Kadian, Ahmad Al-Dahle, Aiesha  
534 Letman, Akhil Mathur, Alan Schelten, Amy Yang, Angela Fan, et al. The llama 3 herd of models.  
535 *arXiv preprint arXiv:2407.21783*, 2024.

537 Yuxin Fang, Wen Wang, Binhui Xie, Quan Sun, Ledell Wu, Xinggang Wang, Tiejun Huang, Xinlong  
538 Wang, and Yue Cao. Eva: Exploring the limits of masked visual representation learning at scale.  
539 In *Proceedings of the IEEE/CVF Conference on Computer Vision and Pattern Recognition*, pp.  
19358–19369, 2023.

540 Sreyan Ghosh, Zhifeng Kong, Sonal Kumar, S Sakshi, Jaehyeon Kim, Wei Ping, Rafael Valle, Di-  
 541 nesh Manocha, and Bryan Catanzaro. Audio flamingo 2: An audio-language model with long-  
 542 audio understanding and expert reasoning abilities. In *Forty-second International Conference on*  
 543 *Machine Learning*, 2025.

544 Arushi Goel, Sreyan Ghosh, Jaehyeon Kim, Sonal Kumar, Zhifeng Kong, Sang-gil Lee, Chao-  
 545 Han Huck Yang, Ramani Duraiswami, Dinesh Manocha, Rafael Valle, et al. Audio flamingo  
 546 3: Advancing audio intelligence with fully open large audio language models. *arXiv preprint*  
 547 *arXiv:2507.08128*, 2025.

548 Haiyang Guo, Fanhu Zeng, Ziwei Xiang, Fei Zhu, Da-Han Wang, Xu-Yao Zhang, and Cheng-Lin  
 549 Liu. HiDe-LLaVA: Hierarchical decoupling for continual instruction tuning of multimodal large  
 550 language model. In *Proceedings of the 63rd Annual Meeting of the Association for Compu-  
 551 tational Linguistics (Volume 1: Long Papers)*, pp. 13572–13586. Association for Computational  
 552 Linguistics, 2025.

553 Jinghan He, Haiyun Guo, Ming Tang, and Jinqiao Wang. Continual instruction tuning for large  
 554 multimodal models. *arXiv preprint arXiv:2311.16206*, 2023.

555 Dan Hendrycks and Kevin Gimpel. Gaussian error linear units (gelus). *arXiv preprint*  
 556 *arXiv:1606.08415*, 2016.

557 Edward J Hu, yelong shen, Phillip Wallis, Zeyuan Allen-Zhu, Yuanzhi Li, Shean Wang, Lu Wang,  
 558 and Weizhu Chen. LoRA: Low-rank adaptation of large language models. In *International Con-  
 559 ference on Learning Representations*, 2022.

560 Tianyu Huai, Jie Zhou, Xingjiao Wu, Qin Chen, Qingchun Bai, Ze Zhou, and Liang He. Cl-moe:  
 561 Enhancing multimodal large language model with dual momentum mixture-of-experts for contin-  
 562 ual visual question answering. In *Proceedings of the Computer Vision and Pattern Recognition*  
 563 Conference, pp. 19608–19617, 2025.

564 Chris Dongjoo Kim, Byeongchang Kim, Hyunmin Lee, and Gunhee Kim. Audiocaps: Generating  
 565 captions for audios in the wild. In *Proceedings of the 2019 Conference of the North American*  
 566 *Chapter of the Association for Computational Linguistics: Human Language Technologies, Vol-  
 567 ume 1 (Long and Short Papers)*, pp. 119–132, 2019.

568 Sanghwan Kim, Lorenzo Noci, Antonio Orvieto, and Thomas Hofmann. Achieving a better  
 569 stability-plasticity trade-off via auxiliary networks in continual learning. In *Proceedings of the*  
 570 *IEEE/CVF Conference on Computer Vision and Pattern Recognition*, pp. 11930–11939, 2023.

571 James Kirkpatrick, Razvan Pascanu, Neil Rabinowitz, Joel Veness, Guillaume Desjardins, Andrei A  
 572 Rusu, Kieran Milan, John Quan, Tiago Ramalho, Agnieszka Grabska-Barwinska, et al. Overcom-  
 573 ing catastrophic forgetting in neural networks. *Proceedings of the national academy of sciences*,  
 574 114(13):3521–3526, 2017.

575 Zhifeng Kong, Arushi Goel, Rohan Badlani, Wei Ping, Rafael Valle, and Bryan Catanzaro. Audio  
 576 flamingo: A novel audio language model with few-shot learning and dialogue abilities. In *Forty-  
 577 first International Conference on Machine Learning*, 2024.

578 Dongxu Li, Junnan Li, Hung Le, Guangsen Wang, Silvio Savarese, and Steven CH Hoi. Lavis: A  
 579 library for language-vision intelligence. *arXiv preprint arXiv:2209.09019*, 2022a.

580 Junnan Li, Dongxu Li, Caiming Xiong, and Steven Hoi. Blip: Bootstrapping language-image pre-  
 581 training for unified vision-language understanding and generation. In *International conference on*  
 582 *machine learning*, pp. 12888–12900. PMLR, 2022b.

583 Junnan Li, Dongxu Li, Silvio Savarese, and Steven Hoi. Blip-2: Bootstrapping language-image  
 584 pre-training with frozen image encoders and large language models. In *International conference*  
 585 *on machine learning*, pp. 19730–19742. PMLR, 2023.

586 Mei Li, Yuxiang Lu, Qinyan Dai, Suizhi Huang, Yue Ding, and Hongtao Lu. BECAME: Bayesian  
 587 continual learning with adaptive model merging. In *Forty-second International Conference on*  
 588 *Machine Learning (ICML)*, 2025.

594 Zhizhong Li and Derek Hoiem. Learning without forgetting. *IEEE transactions on pattern analysis*  
 595 and machine intelligence

596, 40(12):2935–2947, 2017.

597 Samuel Lipping, Parthasarathy Sudarsanam, Konstantinos Drossos, and Tuomas Virtanen. Clotho-  
 598 aqa: A crowdsourced dataset for audio question answering. In *2022 30th European Signal Pro-  
 599 cessing Conference (EUSIPCO)*, pp. 1140–1144. IEEE, 2022.

600 Haotian Liu, Chunyuan Li, Qingyang Wu, and Yong Jae Lee. Visual instruction tuning. *Advances*  
 601 in neural information processing systems

602, 36, 2023.

603 Haotian Liu, Chunyuan Li, Yuheng Li, and Yong Jae Lee. Improved baselines with visual instruction  
 604 tuning. In *Proceedings of the IEEE/CVF Conference on Computer Vision and Pattern Recog-  
 605 nition*, pp. 26296–26306, 2024.

606 David Lopez-Paz and Marc’Aurelio Ranzato. Gradient episodic memory for continual learning.  
 607 *Advances in neural information processing systems*

608, 30, 2017.

609 Ilya Loshchilov and Frank Hutter. Decoupled weight decay regularization. In *International Confer-  
 610 ence on Learning Representations*, 2019.

611 Kenneth Marino, Mohammad Rastegari, Ali Farhadi, and Roozbeh Mottaghi. Ok-vqa: A visual  
 612 question answering benchmark requiring external knowledge. In *Proceedings of the IEEE/CVF*  

613 conference on computer vision and pattern recognition

614, pp. 3195–3204, 2019.

615 Swaroop Mishra, Daniel Khashabi, Chitta Baral, and Hannaneh Hajishirzi. Cross-task generalization  
 616 via natural language crowdsourcing instructions. In *60th Annual Meeting of the Association for*  

617 *Computational Linguistics, ACL 2022*, pp. 3470–3487. Association for Computational Linguistics

618 (ACL), 2022.

619 Shentong Mo, Weiguo Pian, and Yapeng Tian. Class-incremental grouping network for continual  
 620 audio-visual learning. In *Proceedings of the IEEE/CVF International Conference on Computer*  

621 *Vision*, pp. 7788–7798, 2023.

622 Augustus Odena, Christopher Olah, and Jonathon Shlens. Conditional image synthesis with aux-  
 623 illiary classifier gans. In *International conference on machine learning*, pp. 2642–2651. PMLR,  
 625 2017.

626 Oleksiy Ostapenko, Mihai Puscas, Tassilo Klein, Patrick Jahnichen, and Moin Nabi. Learning to  
 627 remember: A synaptic plasticity driven framework for continual learning. In *Proceedings of the*  

628 *IEEE/CVF conference on computer vision and pattern recognition*, pp. 11321–11329, 2019.

629 Artemis Panagopoulou, Le Xue, Ning Yu, Junnan Li, Dongxu Li, Shafiq Joty, Ran Xu, Silvio  
 630 Savarese, Caiming Xiong, and Juan Carlos Niebles. X-instructblip: A framework for aligning  
 631 x-modal instruction-aware representations to llms and emergent cross-modal reasoning. *arXiv*  

632 preprint arXiv:2311.18799, 2023.

633 Adam Paszke, Sam Gross, Francisco Massa, Adam Lerer, James Bradbury, Gregory Chanan, Trevor  
 634 Killeen, Zeming Lin, Natalia Gimelshein, Luca Antiga, et al. Pytorch: An imperative style, high-  
 635 performance deep learning library. *Advances in neural information processing systems*

636, 32, 2019.

637 Weiguo Pian, Shentong Mo, Yunhui Guo, and Yapeng Tian. Audio-visual class-incremental learn-  
 638 ing. In *Proceedings of the IEEE/CVF International Conference on Computer Vision*, pp. 7799–  
 639 7811, 2023.

640 Weiguo Pian, Yiyang Nan, Shijian Deng, Shentong Mo, Yunhui Guo, and Yapeng Tian. Continual  
 641 audio-visual sound separation. In *The Thirty-eighth Annual Conference on Neural Information*  

642 *Processing Systems*, 2024.

643 Alec Radford, Jong Wook Kim, Chris Hallacy, Aditya Ramesh, Gabriel Goh, Sandhini Agarwal,  
 644 Girish Sastry, Amanda Askell, Pamela Mishkin, Jack Clark, et al. Learning transferable visual  
 645 models from natural language supervision. In *International conference on machine learning*, pp.  
 646 8748–8763. PMLR, 2021.

648 Sylvestre-Alvise Rebuffi, Alexander Kolesnikov, Georg Sperl, and Christoph H Lampert. icarl:  
 649 Incremental classifier and representation learning. In *Proceedings of the IEEE conference on*  
 650 *Computer Vision and Pattern Recognition*, pp. 2001–2010, 2017.

651

652 Zechao Sun, Haolin Jin, Weitong Chen, and Luping Zhou. Awf: Adaptive weight fusion for en-  
 653 hanced class incremental semantic segmentation. *arXiv preprint arXiv:2409.08516*, 2024.

654

655 Ramakrishna Vedantam, C Lawrence Zitnick, and Devi Parikh. Cider: Consensus-based image  
 656 description evaluation. In *Proceedings of the IEEE conference on computer vision and pattern*  
 657 *recognition*, pp. 4566–4575, 2015.

658

659 Peng Wang, Shuai Bai, Sinan Tan, Shijie Wang, Zhihao Fan, Jinze Bai, Keqin Chen, Xuejing Liu,  
 660 Jialin Wang, Wenbin Ge, et al. Qwen2-vl: Enhancing vision-language model’s perception of the  
 661 world at any resolution. *arXiv preprint arXiv:2409.12191*, 2024.

662

663 Jia-Wen Xiao, Chang-Bin Zhang, Jiekang Feng, Xialei Liu, Joost van de Weijer, and Ming-Ming  
 664 Cheng. Endpoints weight fusion for class incremental semantic segmentation. In *Proceedings of*  
 665 *the IEEE/CVF Conference on Computer Vision and Pattern Recognition*, pp. 7204–7213, 2023.

666

667 Dejing Xu, Zhou Zhao, Jun Xiao, Fei Wu, Hanwang Zhang, Xiangnan He, and Yueting Zhuang.  
 668 Video question answering via gradually refined attention over appearance and motion. In *Pro-  
 669 ceedings of the 25th ACM international conference on Multimedia*, pp. 1645–1653, 2017.

670

671 Jun Xu, Tao Mei, Ting Yao, and Yong Rui. Msr-vtt: A large video description dataset for bridging  
 672 video and language. In *Proceedings of the IEEE conference on computer vision and pattern*  
 673 *recognition*, pp. 5288–5296, 2016.

674

675 Peter Young, Alice Lai, Micah Hodosh, and Julia Hockenmaier. From image descriptions to visual  
 676 denotations: New similarity metrics for semantic inference over event descriptions. *TACL*, 2:  
 677 67–78, 2014.

678

679 Jiazu Yu, Haomiao Xiong, Lu Zhang, Haiwen Diao, Yunzhi Zhuge, Lanqing HONG, Dong Wang,  
 680 Huchuan Lu, You He, and Long Chen. LLMs can evolve continually on modality for x-modal  
 681 reasoning. In *The Thirty-eighth Annual Conference on Neural Information Processing Systems*,  
 682 2024.

683

684 Fanhu Zeng, Fei Zhu, Haiyang Guo, Xu-Yao Zhang, and Cheng-Lin Liu. Modalprompt: Dual-  
 685 modality guided prompt for continual learning of large multimodal models. *arXiv preprint*  
 686 *arXiv:2410.05849*, 2024.

687

688 Boqiang Zhang, Kehan Li, Zesen Cheng, Zhiqiang Hu, Yuqian Yuan, Guanzheng Chen, Sicong  
 689 Leng, Yuming Jiang, Hang Zhang, Xin Li, et al. Videollama 3: Frontier multimodal foundation  
 690 models for image and video understanding. *arXiv preprint arXiv:2501.13106*, 2025.

691

692 Hang Zhang, Xin Li, and Lidong Bing. Video-LLaMA: An instruction-tuned audio-visual language  
 693 model for video understanding. In *Proceedings of the 2023 Conference on Empirical Methods in*  
 694 *Natural Language Processing: System Demonstrations*, pp. 543–553, 2023a.

695

696

697 Hang Zhang, Xin Li, and Lidong Bing. Video-llama: An instruction-tuned audio-visual language  
 698 model for video understanding. *arXiv preprint arXiv:2306.02858*, 2023b.

699

700 Junhao Zheng, Qianli Ma, Zhen Liu, Binquan Wu, and Huawen Feng. Beyond anti-forgetting:  
 701 Multimodal continual instruction tuning with positive forward transfer. *arXiv preprint*  
*arXiv:2401.09181*, 2024.

702 **A APPENDIX**  
703

704	<b>A.1 Implementation Details</b> . . . . .	14
705	<b>A.2 Overall Algorithm of MoInCL</b> . . . . .	14
706	<b>A.3 Three-Round QA Pairs Generation from Captions</b> . . . . .	14
707	<b>A.4 Dataset Details</b> . . . . .	15
708	<b>A.5 Distinction from Existing Methods</b> . . . . .	16
709	<b>A.6 Analysis on the Computational Cost</b> . . . . .	16
710	<b>A.7 Task Transfer Effectiveness</b> . . . . .	16
711	<b>A.8 Experimental Results on Additional Task Orders</b> . . . . .	17
712	<b>A.9 Upper Bound Results</b> . . . . .	17
713	<b>A.10 Detailed Results of Each Task in Both Orders</b> . . . . .	18
714	<b>A.11 Qualitative Analysis</b> . . . . .	18
715	<b>A.12 Disclosure of the Use of Large Language Models (LLMs)</b> . . . . .	18

721 In this appendix, we provide implementation details in Sec. A.1, the overall algorithm of our pro-  
722 posed method in Sec. A.2, and the process of generating three-round QA pairs from captions in  
723 Sec. A.3. We also include dataset details, distinction from existing methods in Sec. A.4 and A.5,  
724 respectively. Furthermore, we analyze the computation cost and transfer effectiveness between tasks  
725 in Sec. A.6 and A.7. Experimental results on additional task orders, upper bound results, detailed  
726 results of each task, and qualitative analysis are provided in Sec. A.8, A.9, A.10, and A.11, respec-  
727 tively. Finally, we disclose the use of large language models (LLM) in this paper in Sec. A.12.

728  
729 **A.1 IMPLEMENTATION DETAILS**

730 We implement our experiments using Pytorch (Paszke et al., 2019) and LaVIS (Li et al., 2022a)  
731 framework. For the LLM component of the Multimodal Large Language Model (MLLM), we adopt  
732 the Llama-3.2-1B-Instruct (Dubey et al., 2024) architecture and initialize it with pre-trained par-  
733 ameters at the start of the first task. Following the implementation in (Panagopoulou et al., 2023), we  
734 apply the EVA-CLIP-ViT-G/14 (Fang et al., 2023) as the Image Encoder and Video Encoder, and  
735 the BEAT<sub>3iter3</sub> (Chen et al., 2023) as the Audio Encoder. Each video input consists of 4 frames,  
736 and the audio input also consists of 4 frames with the sampling rate of 11kHz. For the video and  
737 audio modalities, the Video Encoder and Audio Encoder process each frame individually and then  
738 concatenate the encoded patches from all frames, following the approach in (Panagopoulou et al.,  
739 2023). For the Image Projection, we use a two-layers MLP with the GELU (Hendrycks & Gimpel,  
740 2016) activation function. For the Video and Audio Projection, both of them include a single convo-  
741 lutional layer as a pooling layer to reduce the total number of patches, followed by a two-layers MLP  
742 with the GELU activation function. All the modalities’ projection modules are initialized randomly  
743 in both our MoInCL and baselines methods, and train them from scratch. For each task, we train  
744 the model using the AdamW (Loshchilov & Hutter, 2019) optimizer with an initial learning rate of  
745 1e-5, adjusted using the cosine decay strategy, and a weight decay of 5e-2. We train our proposed  
746 MoInCL and all baseline methods on a NVIDIA RTX A6000 Ada GPU. During the training of our  
747 approach, the pure text instructions in the Instruction-based Knowledge Distillation (IKD) constraint  
748 are randomly sampled from the Natural Instructions (Mishra et al., 2022) dataset.

749 **A.2 OVERALL ALGORITHM OF MOINCL**  
750

751 The overall algorithm of our proposed MoInCL is presented in Alg. 1.

752 **A.3 THREE-ROUND QA PAIRS GENERATION FROM CAPTIONS**  
753

754 Inspired by the question answering text generation process in (Panagopoulou et al., 2023), we adopt  
755 a similar three-round QA pair generation process from captions in our proposed Pseudo Targets

756 **Algorithm 1** Training of MoInCL on task  $\mathcal{T}_i$ 


---

757 **Require:** Old model  $\mathcal{F}_{\Theta_{i-1}}$ , training set  $\mathcal{D}_i$ , pure text instruction set  $\mathcal{I}$ , current modality  $M_i$ , cur-  
 758    rent task type  $P_i$ , learned modalities set  $LM$ , learned task type for the current modality  $LT_{M_i}$   
 759    (only if  $M_i \in LM$ ), learning rate  $\eta$ , scalars  $\lambda_i, \lambda'_i, \alpha_i$

760   1: Initialize current model  $\mathcal{F}_{\Theta_i}$  from  $\mathcal{F}_{\Theta_{i-1}}$

761   2: **if**  $M_i \notin LM$  **then**

762    3:  $\{\} \rightarrow LT_{M_i}$

763   4: **end if**

764   5: **while** not converged **do**

765     6: Sample data  $(\mathbf{x}, \mathbf{t}, \mathbf{y}) \sim \mathcal{D}_i$

766     7:  $\mathcal{L} = \mathcal{L}_{CE}(\mathcal{F}_{\Theta_i}(\mathbf{x}, \mathbf{t}) || \mathbf{y})$

767     8: **if**  $M_i \in LM$  and  $LT_{M_i} \neq \emptyset$  **then**

768       9:  $\tilde{\mathbf{t}}, \tilde{\mathbf{y}} = PTGM(\mathbf{x}, \mathbf{y}, p)$ , s.t.  $p \in LT_{M_i}$

769       10:  $\hat{\mathbf{y}}' = \mathcal{F}_{\Theta_i}(\mathbf{x}, \tilde{\mathbf{t}}), \hat{\mathbf{y}}'_o = \mathcal{F}_{\Theta_{i-1}}(\mathbf{x}, \tilde{\mathbf{t}})$

770       11:  $\mathcal{L}_{p.} = \lambda_i \mathcal{L}_{CE}(\hat{\mathbf{y}}' || \tilde{\mathbf{y}}) + \lambda'_i \mathcal{L}_{KL}(\hat{\mathbf{y}}' || \hat{\mathbf{y}}'_o)$

771       12:  $\mathcal{L} = \mathcal{L} + \mathcal{L}_{p.}$

772       13: **end if**

773       14: Sample instruction data  $\mathbf{t}' \sim \mathcal{I}$

774       15:  $\mathcal{L}_{ins.} = \mathcal{L}_{KL}(f_{\Theta_i}(\mathbf{t}') || f_{\Theta_{i-1}}(\mathbf{t}'))$

775       16:  $\mathcal{L} = \mathcal{L} + \mathcal{L}_{ins.}$

776       17:  $\Theta_i \leftarrow \Theta_i - \eta \nabla \mathcal{L}$

777       18:  $\theta_i \leftarrow \alpha_i \theta_i + (1 - \alpha_i) \theta_{i-1}$

778     19: **end while**

---

780 Generation Module (PTGM). Given a caption from the dataset of the current captioning task  $\mathcal{T}_i$ ,  
 781 the objective is to generate a QA pair to address the task type shift problem when training on a  
 782 captioning task within a seen modality. This process relies entirely on prompt engineering, where  
 783 the caption is used as input to the pre-trained Large Language Model (LLM) component of our  
 784 Multimodal Large Language Model (MLLM). Please note that, the LLM component employed in  
 785 this process uses pre-trained weights, *i.e.*, the weights that are not fine-tuned on our incremental  
 786 tasks.

787 In Round 1, the LLM takes an input with the format of: *Given the  $M_i$  context: "y",*  
 788 *generate a potential short answer from it. Provide just one or*  
 789 *two words. The answer words should be strictly selected from the*  
 790 *context. Provide only the answer, nothing else. Answer:*, where  $M_i$  is  
 791 the modality of the task  $\mathcal{T}_i$ ,  $y$  denotes the sampled caption text. And the output of the LLM is used  
 792 as the temporal short answer  $\tilde{y}$ .

793 In Round 2, the LLM takes the following prompt as input: *Given the  $M_i$  context:*  
 794 *"y" and the answer: "tilde y", generate a question for the answer that*  
 795 *can be inferred from the context. Provide only one question and*  
 796 *nothing else. Question:*. The output of the LLM in Round 2 is the question we aim to  
 797 generate, which is denoted as  $\tilde{t}$ .

798 Finally, in Round 3, the LLM processes the following prompt as input: *Answer the question*  
 799 *using the given context. The answer should be only one or two*  
 800 *words. Context: "y". Question: "tilde t". Answer:*, and generates the final  
 801 short answer  $\tilde{y}$ .

802 Based the above three rounds, the pseudo QA pair is obtained, where  $\tilde{t}$  represents the pseudo ques-  
 803 tion and  $\tilde{y}$  denotes the pseudo answer.

805 **A.4 DATASET DETAILS**

808 In our experiments, we use the AudioCaps, Flickr30K, MSR-VTT, MSVD-QA, Clotho-AQA, and  
 809 OK-VQA datasets for Audio Captioning, Image Captioning, Video Captioning, Video QA, Audio  
 810 QA, and Image QA tasks, respectively. We summarize the details of these data in Tab. 4.

810  
811  
812  
813  
814  
815  
816  
817  
818  
819  
820  
821  
822  
823  
Table 4: Details of the datasets used in our experiments.  
824  
825  
826  
827  
828  
829  
830  
831  
832  
833  
834  
835  
836  
837  
838  
839  
840  
841  
842  
843  
844  
845  
846  
847  
848  
849  
850  
851  
852  
853  
854  
855  
856  
857  
858  
859  
860  
861  
862  
863

Task	Dataset	Total	Sample number		
			Training	Validation	Testing
Image Captioning	Flickr30K	31,784	29,783	1,000	1,000
Image QA	OK-VQA	14,055	8,007	1,002	5,046
Audio Captioning	AudioCaps	46,378	44,378	1,000	1,000
Audio QA	Clotho-AQA	10,480	6,181	1,823	2,476
Video Captioning	MSR-VTT	10,000	6,010	1,000	2,990
Video QA	MSVD-QA	50,476	30,904	6,415	13,157

### A.5 DISTINCTION FROM EXISTING METHODS

Our MoInCL introduces two key innovations: 1) a Pseudo Target Generation Module (PTGM) to leverage the text generation capability of the LLM component in the MLLM to address the task type shift challenge in our proposed MICL scenario, and 2) an Instruction-based Knowledge Distillation (IKD) constraint to tackle the modality shift problem in the LLM component of the MLLM.

While existing works also utilize knowledge distillation techniques to preserve knowledge from old tasks, they primarily focus on distilling final outputs or internal features between old and current models by taking same training samples as input, as seen in methods like LwF (Li & Hoiem, 2017) and EWF (Xiao et al., 2023). These approaches do not perform well in our MICL scenario, as they significantly constrain the MLLM’s ability to learn new tasks, particularly in settings with substantial gaps between tasks, such as in our proposed MICL.

In contrast, our IKD leverages pure text instructions as the input to the LLM component for knowledge distillation, avoiding introducing negative impacts on the current training task. This approach allows us to directly distill knowledge of the LLM without imposing additional constraints on the MLLM’s ability to learn new tasks, ensuring that both knowledge preservation and new task learning are achieved effectively in MICL.

As for the weight fusion strategy, we acknowledge that it is not one of our primary technical contributions. However, our experiments demonstrate that this strategy can be seamlessly integrated with PTGM and IKD to further enhance the anti-forgetting capability of our approach. For this reason, we also include the weight fusion strategy in our method.

### A.6 ANALYSIS ON THE COMPUTATIONAL COST

For each experiment, *i.e.*, training a single baseline method or our MoInCL, we use a single RTX A6000 Ada GPU with 48GB of memory. Compared to the pure fine-tuning baseline, the average training time for our MoInCL increases by approximately 40% per epoch, while the inference time remains the same. For example, during training on the audio captioning task with the AudioCaps dataset, pure fine-tuning takes around 45 minutes per epoch, and our method requires approximately 64 minutes per epoch.

### A.7 TASK TRANSFER EFFECTIVENESS

To investigate the mutual impact between different tasks, we evaluate the positive knowledge transfer across tasks that share the same modality or task type. Specifically, we conduct experiments to determine whether training on one task benefits a subsequent task within the same modality or task type. The experimental results are presented in Tab. 5. As shown, transferring the captioning ability from the image captioning task improves the CIDEr score of the video captioning task from 47.12 to 48.03. Similarly, transferring the question-answering capability from the video QA task enhances the accuracy of the audio QA task from 58.28 to 59.94. These results further demonstrate that transferring knowledge from a previous task to a new task with the same task type enhances the performance of this new task. Additionally, the audio QA ability is enhanced by transferring knowledge from the learned audio captioning task, improving accuracy from 58.28 to 61.75. Similarly, positive

864 Table 5: Experimental results on task transfer effectiveness. We evaluate modality transfer effec-  
 865 tiveness within the same task type and task type transfer effectiveness within the same modality.  
 866

Modality Transfer				Task Type Transfer	
Video Cap 47.12	Image Cap → Video Cap 48.03	Audio QA 58.28	Video QA → Audio QA 59.94	Audio QA 58.28	Audio Cap → Audio QA 61.75
Task Type Transfer					
Image QA 35.00	Image Cap → Image QA 36.50	Video Cap 47.12	Video QA → Video Cap 51.25	Image Cap 77.50	Image QA → Image Cap 81.93

870  
 871 Table 6: Experimental results on additional two task orders for different continual learning methods.  
 872 Bold values indicate the best results in each column, while underlined values represent the second-  
 873 best results in each column.  
 874

Methods	Avg. CIDEr ↑	Order 3			Order 4		
		Avg. Acc. ↑	Avg. Forget. ↓	Avg. CIDEr ↑	Avg. Acc. ↑	Avg. Forget. ↓	
Fine-tuning	23.14	<u>41.59</u>	53.18%	46.16	19.94	56.11%	
EWF (Xiao et al., 2023)	<u>35.46</u>	37.10	<u>46.14%</u>	46.92	<u>36.72</u>	<u>29.66%</u>	
PathWeave (Yu et al., 2024)	28.46	40.50	51.73%	<u>47.27</u>	20.54	53.72%	
<b>MoInCL (Ours)</b>	<b>57.18</b>	<b>45.39</b>	<b>13.07%</b>	<b>57.77</b>	<b>40.81</b>	<b>14.93%</b>	
Upper Bound (Joint training)	66.69	48.97	-	66.69	48.97	-	

885 knowledge transfer is observed within the image and video modalities, further demonstrating the  
 886 benefits of transferring knowledge across tasks within the same modality.  
 887

#### 888 A.8 EXPERIMENTAL RESULTS ON ADDITIONAL TASK ORDERS

891 Apart from the random task orders in Sec. 4.2, we also conduct additional experiments to further  
 892 verify the effectiveness and robustness of our proposed MoInCL. Specifically, we construct a new  
 893 random order: **Video Captioning → Image QA → Image Captioning → Video QA → Audio Cap-**  
 894 **tioning → Audio QA**, which we refer to as **Order 3**.

895 Additionally, we also manually create another task order: **Image QA → Video Captioning → Audio**  
 896 **QA → Image Captioning → Video QA → Audio Captioning**, one of the most challenging task  
 897 orders. This task order enforces frequent alternation between task types, following the pattern:  
 898 **QA → Captioning → QA → Captioning → QA → Captioning**, which ensures no two tasks of the  
 899 same task type appear consecutively. Moreover, this order also introduces more frequent modality  
 900 shifts, avoiding repetition of the same modality in adjacent tasks. This setting helps mitigate task-  
 901 recency bias and offers a more rigorous evaluation of each method’s ability to generalize under  
 902 highly dynamic conditions. We refer to this extreme task order as **Order 4**.

903 The experimental results on these two new task orders are reported in Tab. 6. As shown, our method  
 904 consistently achieves significant improvements over the baseline methods. Furthermore, its perfor-  
 905 mance remains in line with the results on the original task orders, further highlighting the stability  
 906 and robustness of our approach.  
 907

908 Table 7: Experimental results of the Upper Bound (joint training) on each task.  
 909

Methods	Flickr30k	MSR-VTT	MSVD-QA	OK-VQA	AudioCaps	Clotho-AQA
Upper Bound (Joint training)	80.24	54.76	48.54	38.16	65.07	60.22

#### 915 A.9 UPPER BOUND RESULTS

916 917 We present the testing results of the Upper Bound (joint training) on each task in Tab. 7.  
 918

918 A.10 DETAILED RESULTS OF EACH TASK IN BOTH ORDERS  
919

920 We present the forgetting ratio of each task in both orders in Tab. 8 and 9, from which we can see  
921 that, our method outperforms baseline methods significantly, further demonstrating the superiority  
922 of our proposed method in mitigating the catastrophic forgetting in our proposed MICL scenario.

923 We also present the detailed testing results for each task across the incremental steps in both orders  
924 in Tab. 10 and 11. These results show that our proposed MoInCL exhibits less performance  
925 drop compared to the baseline methods, demonstrating its superior ability to address catastrophic  
926 forgetting in the proposed Modality-Inconsistent Continual Learning (MICL) scenario.  
927

928 Table 8: Forgetting ratio of each task in Order 1. Bold values denote the best results in each column,  
929 while underlined values indicate the second-best results in each column.

Methods	Forgetting Ratio ↓					
	AudioCaps	Flickr30k	MSVD-QA	Clotho-AQA	OK-VQA	MSR-VTT
Fine-tuning	57.51%	85.04%	<u>51.33%</u>	7.15%	4.81%	0.00%
LwF (Li & Hoiem, 2017)	<u>54.79%</u>	72.52%	59.32%	2.76%	6.92%	0.00%
EWC (Kirkpatrick et al., 2017)	62.47%	<u>46.55%</u>	61.55%	9.95%	13.42%	0.00%
EWF (Xiao et al., 2023)	69.65%	92.51%	79.07%	0.47%	<u>1.03%</u>	0.00%
PathWeave (Yu et al., 2024)	75.49%	58.16%	61.74%	16.25%	<u>10.18%</u>	0.00%
BECAKE (Li et al., 2025)	72.82%	92.70%	66.04%	<u>-0.13%</u>	3.36%	0.00%
<b>MoInCL (Ours)</b>	<b>27.52%</b>	<b>9.18%</b>	<b>36.58%</b>	<u>0.07%</u>	<b>-2.28%</b>	0.00%

938 Table 9: Forgetting ratio of each task in Order 2. Bold values denote the best results in each column,  
939 while underlined values indicate the second-best results in each column.

Methods	Forgetting Ratio ↓					
	Flickr30k	MSR-VTT	MSVD-QA	OK-VQA	AudioCaps	Clotho-AQA
Fine-tuning	93.02%	85.72%	31.23%	49.77%	68.06%	0.00%
LwF (Li & Hoiem, 2017)	91.20%	85.83%	31.51%	40.07%	60.60%	0.00%
EWC (Kirkpatrick et al., 2017)	91.08%	92.21%	40.49%	37.91%	70.31%	0.00%
EWF (Xiao et al., 2023)	<u>89.86%</u>	<u>78.28%</u>	<u>6.04%</u>	<u>4.15%</u>	<u>54.89%</u>	0.00%
PathWeave (Yu et al., 2024)	92.42%	87.54%	25.67%	35.51%	66.22%	0.00%
BECAKE (Li et al., 2025)	90.50%	80.31%	15.48%	9.92%	74.29%	0.00%
<b>MoInCL (Ours)</b>	<b>22.04%</b>	<b>2.25%</b>	<b>2.60%</b>	<b>3.33%</b>	<b>14.43%</b>	0.00%

950 A.11 QUALITATIVE ANALYSIS  
951

952 We present the qualitative results of the Fine-tuning, LwF (Li & Hoiem, 2017), EWC (Kirkpatrick  
953 et al., 2017), EWF (Xiao et al., 2023), PathWeave (Yu et al., 2024), and our MoInCL in Fig. 3, 4, 5,  
954 6, 7, and 8, respectively. From these results, we can see that our MoInCL can generate better results  
955 with the incremental step increases, demonstrating the better capability in mitigating the catastrophic  
956 forgetting problem in our proposed Modality-Inconsistent Continual Learning (MICL) scenario.  
957

958 A.12 DISCLOSURE OF THE USE OF LARGE LANGUAGE MODELS (LLMs)  
959

960 The authors used ChatGPT (Achiam et al., 2023) for minor grammar and language refinements. All  
961 technical content, analysis, and writing were produced by the authors.

962  
963  
964  
965  
966  
967  
968  
969  
970  
971

972  
973  
974  
975  
976  
977  
978  
979  
980  
981  
982  
983

Table 10: Detailed testing results for each task across the incremental steps in Order 1. The evaluation metric used for the AudioCaps, Flickr30K, and MSR-VTT datasets is CIDEr score, while that for the MSVD-QA, Clotho-AQA, and OK-VQA datasets is accuracy.

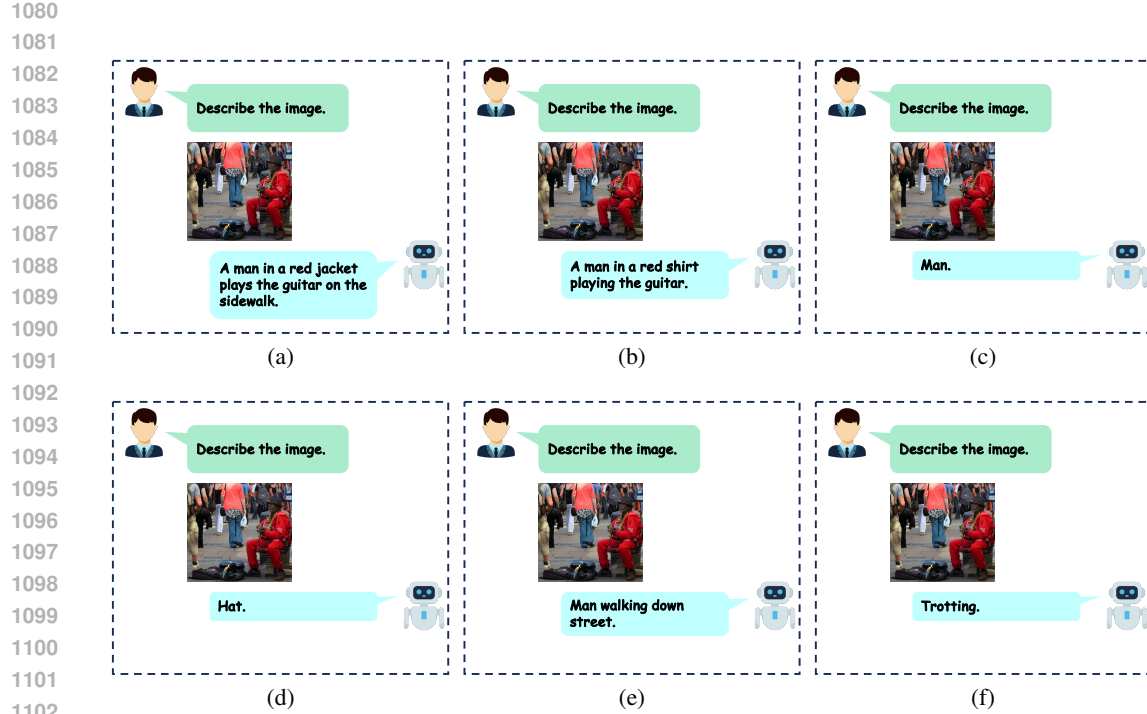
		AudioCaps	Flickr30K	MSVD-QA	Clotho-AQA	OK-VQA	MSR-VTT
985 986 987 988 989 990	Fine-tuning	Step 1	57.66	-	-	-	-
		Step 2	26.42	85.83	-	-	-
		Step 3	8.34	30.83	47.67	-	-
		Step 4	4.28	21.89	44.52	62.64	-
		Step 5	4.06	6.49	39.36	57.51	42.41
		Step 6	24.50	12.84	23.20	58.16	40.37
991 992 993 994 995 996	LwF (Li & Hoiem, 2017)	Step 1	57.66	-	-	-	-
		Step 2	26.32	86.97	-	-	-
		Step 3	4.61	30.38	47.47	-	-
		Step 4	0.04	15.96	42.08	63.13	-
		Step 5	1.18	6.36	36.16	59.85	42.89
		Step 6	26.07	23.90	19.31	61.39	39.92
997 998 999 1000 1001 1002	EWC (Kirkpatrick et al., 2017)	Step 1	57.66	-	-	-	-
		Step 2	38.59	85.27	-	-	-
		Step 3	5.67	25.23	46.03	-	-
		Step 4	2.04	14.21	43.78	63.29	-
		Step 5	3.85	6.31	38.85	56.70	42.09
		Step 6	21.64	45.58	17.70	56.99	36.44
1003 1004 1005 1006 1007 1008	EWF (Xiao et al., 2023)	Step 1	57.66	-	-	-	-
		Step 2	49.84	82.73	-	-	-
		Step 3	38.01	71.03	44.33	-	-
		Step 4	14.19	65.28	44.22	59.69	-
		Step 5	15.48	6.08	43.98	59.53	40.75
		Step 6	17.50	6.20	9.28	59.41	40.33
1009 1010 1011 1012 1013 1014	PathWeave (Yu et al., 2024)	Step 1	59.86	-	-	-	-
		Step 2	13.54	82.32	-	-	-
		Step 3	2.95	12.02	46.00	-	-
		Step 4	0.54	9.07	37.28	63.13	-
		Step 5	4.19	6.26	28.97	57.84	42.42
		Step 6	14.67	34.44	17.60	52.87	38.10
1015 1016 1017 1018 1019 1020	BECAME (Li et al., 2025)	Step 1	57.66	-	-	-	-
		Step 2	55.71	81.46	-	-	-
		Step 3	18.34	63.77	45.61	-	-
		Step 4	5.81	54.34	45.31	60.18	-
		Step 5	9.43	6.04	40.39	59.13	41.13
		Step 6	15.67	5.95	15.49	60.26	39.75
1021 1022 1023 1024 1025	MoInCL (Ours)	Step 1	57.66	-	-	-	-
		Step 2	56.58	81.15	-	-	-
		Step 3	56.51	82.71	43.38	-	-
		Step 4	43.44	81.91	43.43	57.71	-
		Step 5	43.01	74.19	43.51	57.51	40.75
		Step 6	41.79	73.70	27.51	57.67	41.68
Upper Bound (Joint training)		65.07	80.24	48.54	60.22	38.16	54.76

1026  
1027  
1028  
1029  
1030  
1031  
1032  
1033

1034 Table 11: Detailed testing results for each task across the incremental steps in Order 2. The evalua-  
1035 tion metric used for the AudioCaps, Flickr30K, and MSR-VTT datasets is CIDEr score, while that  
1036 for the MSVD-QA, Clotho-AQA, and OK-VQA datasets is accuracy.  
1037

		Flickr30K	MSR-VTT	MSVD-QA	OK-VQA	AudioCaps	Clotho-AQA
Fine-tuning	Step 1	77.50	-	-	-	-	-
	Step 2	64.04	48.03	-	-	-	-
	Step 3	12.12	8.64	46.20	-	-	-
	Step 4	5.86	8.23	39.38	37.13	-	-
	Step 5	9.63	14.05	24.91	17.24	63.19	-
	Step 6	5.41	6.86	31.77	18.65	20.18	60.62
LwF (Li & Hoiem, 2017)	Step 1	77.50	-	-	-	-	-
	Step 2	53.87	48.70	-	-	-	-
	Step 3	10.20	7.80	47.64	-	-	-
	Step 4	7.41	8.44	37.14	36.51	-	-
	Step 5	12.51	18.08	31.44	19.47	59.37	-
	Step 6	6.82	6.90	32.63	21.88	23.39	61.87
EWC (Kirkpatrick et al., 2017)	Step 1	77.50	-	-	-	-	-
	Step 2	62.65	47.73	-	-	-	-
	Step 3	10.45	9.66	45.79	-	-	-
	Step 4	7.19	7.85	37.42	35.90	-	-
	Step 5	12.10	4.24	27.59	21.09	64.40	-
	Step 6	6.91	3.72	27.25	22.29	19.12	63.41
EWF (Xiao et al., 2023)	Step 1	77.50	-	-	-	-	-
	Step 2	69.16	45.30	-	-	-	-
	Step 3	56.10	9.69	45.33	-	-	-
	Step 4	8.26	9.85	44.74	34.95	-	-
	Step 5	8.04	10.24	43.31	33.10	53.36	-
	Step 6	7.86	9.84	42.59	33.50	24.07	61.47
PathWeave (Yu et al., 2024)	Step 1	77.22	-	-	-	-	-
	Step 2	53.60	50.01	-	-	-	-
	Step 3	7.36	8.35	47.87	-	-	-
	Step 4	6.99	7.14	41.17	36.38	-	-
	Step 5	8.01	7.86	33.89	22.27	62.90	-
	Step 6	5.85	6.23	35.58	23.46	21.25	64.34
BECAME (Li et al., 2025)	Step 1	77.50	-	-	-	-	-
	Step 2	77.22	47.64	-	-	-	-
	Step 3	52.16	9.82	47.35	-	-	-
	Step 4	7.24	9.59	46.36	34.48	-	-
	Step 5	8.04	8.81	43.11	31.62	58.74	-
	Step 6	7.36	9.38	40.02	31.06	15.10	58.52
MoInCL (Ours)	Step 1	77.50	-	-	-	-	-
	Step 2	73.59	48.03	-	-	-	-
	Step 3	70.88	48.34	43.11	-	-	-
	Step 4	63.32	47.56	42.27	33.35	-	-
	Step 5	61.91	47.78	42.24	33.46	53.79	-
	Step 6	60.42	46.95	41.99	32.24	46.03	61.43
Upper Bound (Joint training)		80.24	54.76	48.54	38.16	65.07	60.22

1071  
1072  
1073  
1074  
1075  
1076  
1077  
1078  
1079



1103 Figure 3: Qualitative results of the Fine-tuning method in Order 2. The sample is randomly selected  
1104 from the test set of Task 1 (Image Captioning). The results are generated using models trained after  
1105 after (a) Task 1, (b) Task 2, (c) Task 3, (d) Task 4, (e) Task 5, and (f) Task 6.



1131 Figure 4: Qualitative results of the LwF (Li & Hoiem, 2017) method in Order 2. The sample is  
1132 randomly selected from the test set of Task 1 (Image Captioning). The results are generated using  
1133 models trained after (a) Task 1, (b) Task 2, (c) Task 3, (d) Task 4, (e) Task 5, and (f) Task 6.

1134

1135

1136

1137

1138

1139

1140

1141

1142

1143

1144

1145

1146

1147

1148

1149

1150

1151

1152

1153

1154

1155

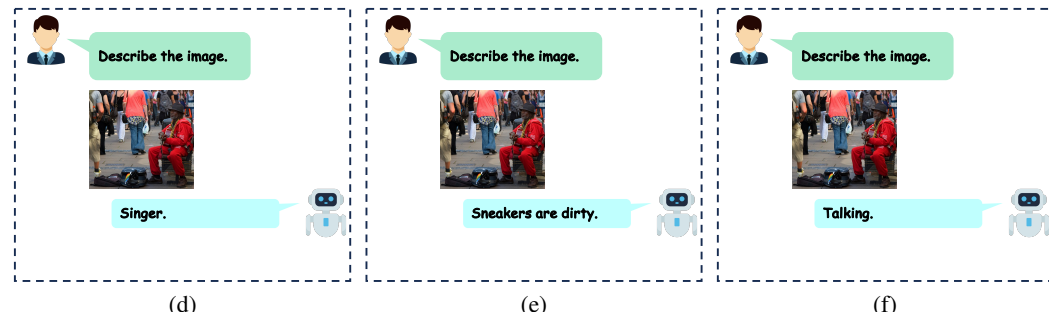
1156



(a)

(b)

(c)



(d)

(e)

(f)

Figure 5: Qualitative results of the EWC (Kirkpatrick et al., 2017) method in Order 2. The sample is randomly selected from the test set of Task 1 (Image Captioning). The results are generated using models trained after (a) Task 1, (b) Task 2, (c) Task 3, (d) Task 4, (e) Task 5, and (f) Task 6.

1160

1161

1162

1163

1164

1165

1166

1167

1168

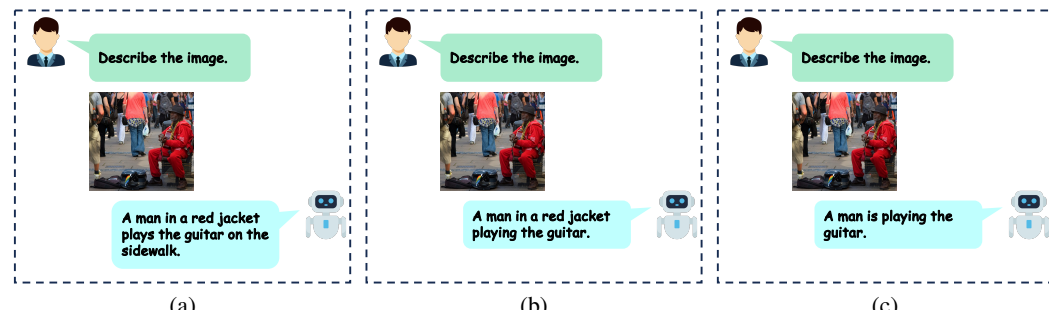
1169

1170

1171

1172

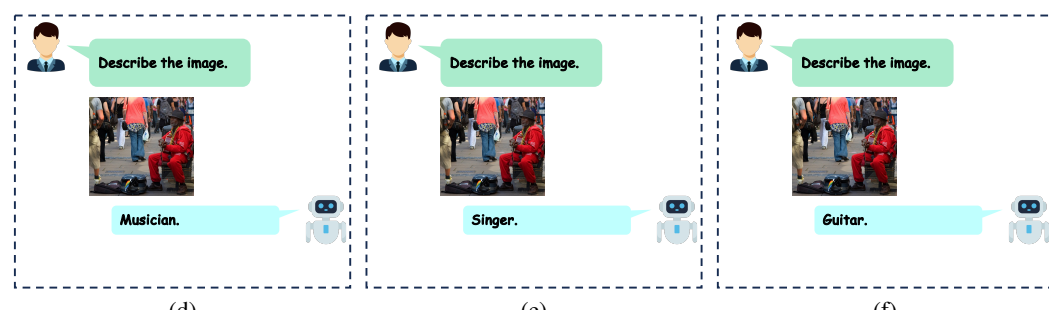
1173



(a)

(b)

(c)



(d)

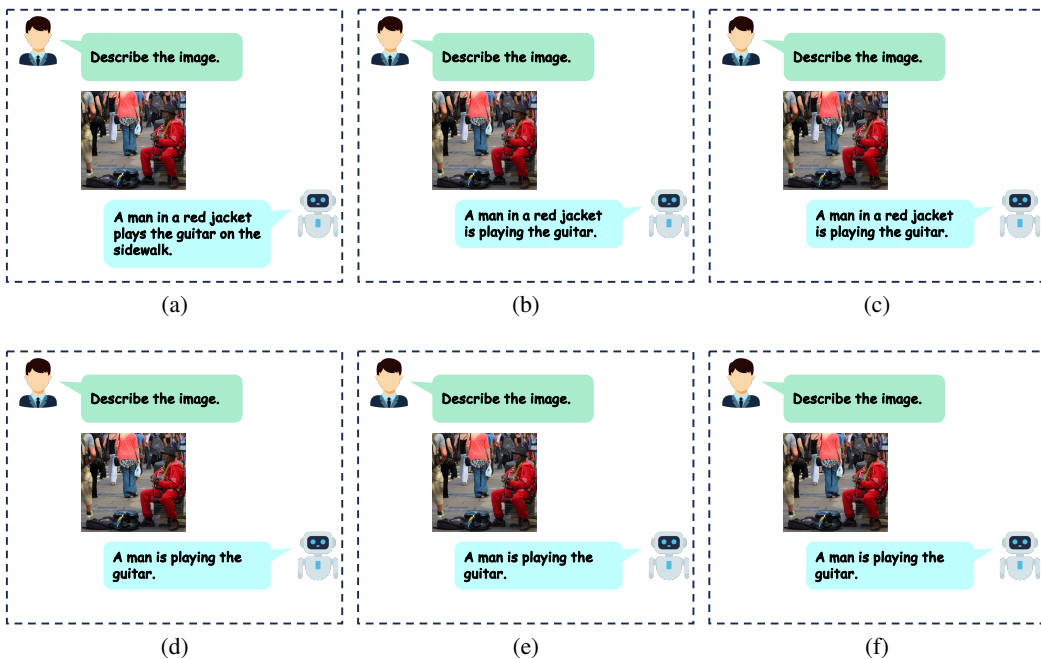
(e)

(f)

Figure 6: Qualitative results of the EWF (Xiao et al., 2023) method in Order 2. The sample is randomly selected from the test set of Task 1 (Image Captioning). The results are generated using models trained after (a) Task 1, (b) Task 2, (c) Task 3, (d) Task 4, (e) Task 5, and (f) Task 6.



1211 Figure 7: Qualitative results of the PathWeave (Yu et al., 2024) method in Order 2. The sample is  
1212 randomly selected from the test set of Task 1 (Image Captioning). The results are generated using  
1213 models trained after (a) Task 1, (b) Task 2, (c) Task 3, (d) Task 4, (e) Task 5, and (f) Task 6.



1238 Figure 8: Qualitative results of our proposed MoInCL in Order 2. The sample is randomly selected  
1239 from the test set of Task 1 (Image Captioning). The results are generated using models trained after  
1240 (a) Task 1, (b) Task 2, (c) Task 3, (d) Task 4, (e) Task 5, and (f) Task 6.